

Supplementary Information

**Spectroscopic capture and reactivity of  $S = 1/2$  nickel(III)-oxygen intermediates in the reaction of a  $\text{Ni}^{\text{II}}$ -salt with  $m\text{CPBA}$ †**

Florian F. Pfaff, Florian Heims, Subrata Kundu, Stefan Mebs, and Kallol Ray\*

Humboldt-Universität zu Berlin, Institut für Chemie, Brook-Taylor-Straße 2, D-12489

\* E-mail: [kallol.ray@chemie.hu-berlin.de](mailto:kallol.ray@chemie.hu-berlin.de)

## Experimental Section

### 1) Materials

Chemicals were purchased from Sigma-Aldrich, Acros, TCI and ABCR and used without further purification unless otherwise mentioned. Anhydrous dichloromethane, acetone, diethylether and anhydrous *n*-hexane were purchased from Carl-Roth GmbH ( $\geq 99.5\%$ ,  $\leq 50$  ppm H<sub>2</sub>O) and degassed by freeze-pump-thaw method prior to use. Metachloroperoxybenzoic acid (*m*CPBA) was purified by washing with pH buffer solution.<sup>[1]</sup> DHA-d<sub>4</sub> was prepared following the published procedure.<sup>[2]</sup>

### 2) Instrumentation and physical methods

Preparation and handling of air sensitive materials were done in a N<sub>2</sub> glove box: OMNI-Lab 2 (VAC) with O<sub>2</sub> and moisture concentrations less than 1 ppm. <sup>1</sup>H NMR spectra were recorded either on a Bruker AV 400 NMR spectrometer or on a Bruker DPX 300 spectrometer. Elemental analyses were performed with a Leco CHNS-932 elemental analyzer. UV/vis spectra were recorded by an Agilent 8453 diode array spectrometer connected with a cryostat from Unisoku Scientific Instruments, Japan.

The analyses of the different substrate oxidations were done by GC-MS/FID (Varian GC/MS 4000). The products of the reactivity studies were identified by comparison of the retention times of the authentic compounds and the quantification of the products were done by using diphenyl ether as an internal standard.

X-band EPR derivative spectra were recorded on a Bruker ELEXSYS E500 spectrometer equipped with the Bruker dual-mode cavity (ER4116DM) and a helium flow cryostat (Oxford Instruments ESR 910). Microwave frequencies were calibrated with a Hewlett-Packard frequency counter (HP5352B), and the field control was calibrated with a Bruker NMR field probe (ER035M). The spectrum was simulated with the program GFIT (by Dr. Eckhard Bill) for the calculation of spectra with effective *g* values and anisotropic line widths (Gaussian line shapes were used).

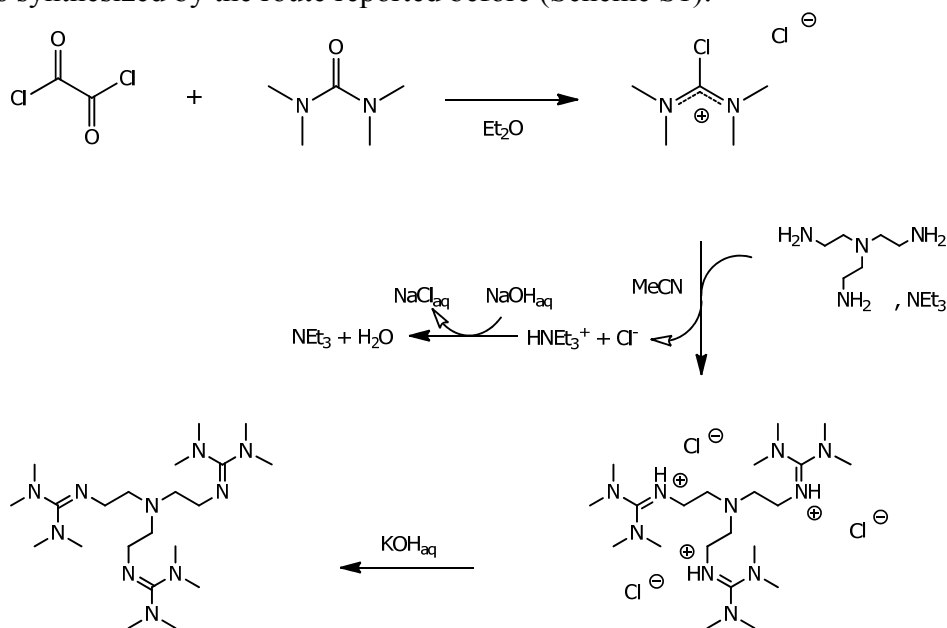
**Crystal Structure Determination.** Data collection was performed at 100 K on a Stoe IPDS 2T diffractometer using Mo-*K*<sub>α</sub> radiation ( $\lambda = 0.71073$  Å). The radiation source was a sealed x-ray tube with graphite monochromator. A multi-scan absorption correction was applied ( $\mu = 0.751$ ,  $T_{\min} = 0.6129$ ,  $T_{\max} = 0.8071$ ,  $R_{\text{int}} = 7.09$ ).<sup>[3]</sup> The structures were solved by direct methods (SHELXS-97) and refined by full matrix least-squares procedures based on  $F^2$  with all measured reflections (SHELXL-97).<sup>[4]</sup> All

non-hydrogen atoms were refined anisotropically. H atoms were introduced in their idealized positions and refined as riding model. The suitability indexes are:  $R_1 = 0.0601$ ,  $wR_2 = 0.1677$ . 68675 reflections were collected, 9845 unique, 8690 observed. Crystal structure of **1-OTf** crystallizes in the space group P 21/c ( $a = 11.9694(2)$  Å,  $b = 15.6473(3)$  Å,  $c = 18.9697(3)$  Å,  $\alpha = 90^\circ$ ,  $\beta = 96.441(1)^\circ$ ,  $\gamma = 90^\circ$ ).

### 3. Synthesis of Ligand and Complex 1-OTf

- **Ligand Synthesis (TMG<sub>3</sub>tren)**

The ligand was synthesized by the route reported before (Scheme S1):<sup>[5]</sup>



Scheme S1 Ligand synthesis

- **Complex Synthesis 1-OTf**

**Synthesis of [Ni(TM<sub>G</sub><sub>3</sub>tren)(OTf)](OTf).** A solution of TMG<sub>3</sub>tren (275 mg) in CH<sub>2</sub>Cl<sub>2</sub>/Toluene (1:2, 10 mL) was added to [Ni(OTf)<sub>2</sub>] (223 mg), and the resultant mixture stirred over 48h under a nitrogen atmosphere. The solution was then filtered to remove the unreacted [Ni(OTf)<sub>2</sub>]. 20 ml of diethyl ether was then added to the resultant filtrate and left overnight. The brown crystals were isolated by filtration, washed with diethyl ether (2 -5 mL), and dried under vacuum. 65 % yield.

Needle shaped crystals were suitable for X-ray diffraction.

Elemental analysis:

	C [%]	H [%]	N [%]	S [%]
Calc.	34.64	6.07	17.56	8.03
Found	34.99	6.06	17.52	7.26

ESI-MS:

$[\text{Ni}^{\text{II}}\text{TMG}(\text{OTf})]^+$ : calc.: 647.2879  
found: 647.2937

$[\text{Ni}^{\text{II}}\text{TMG}(\text{Cl})]^+$ : calc.: 533.3096  
found: 533.3105

The formation of the chloride complex results from the reaction of the triflate complex with the solvent ( $\text{CH}_2\text{Cl}_2$ ) under the ESI-MS conditions.

### 3) Reactivity and Spectroscopy

#### • Oxidation of 1-OTf with *m*CPBA

The reaction was performed at various concentrations between 1 and 50 mM under inert conditions. **1-OTf** was dissolved in dichloromethane (2 mL, yellowish/brown solution) and a solution of meta-chloroperoxybenzoic acid (*m*CPBA, 1eq.) in dichloromethane (0.3 mL) was added at -30 °C. Within 25 minutes the solution turns deep red to form the intermediate **2**. The reaction was followed by UV/vis and EPR spectroscopy. EPR signals were quantified by double integration with a frozen solution of copper(II) acetylacetonate as a standard at 10 K.

**UV/vis investigations** were performed in a quartz cuvette with a long neck and a septum head. The cuvette was filled with a solution of  $[\text{Ni}(\text{TMG}_3\text{tren})(\text{OTf})](\text{OTf})$  and sealed within the glove box and put for the UV/vis cryostat immediately. The temperature was stabilized for 5 minutes while argon overpressure was set within the cuvette. The oxidant was added via a syringe (prepared in the glove box). For kinetic studies, the preformed intermediate was treated with various substrates (10-100 eq.) dissolved in 0.3 mL  $\text{CH}_2\text{Cl}_2$  at -30 °C. The substrate solution was prepared before in the glovebox. The pseudo first order decay of band at 520 nm was monitored by UV/vis spectroscopy.

Samples for **EPR spectroscopy** were prepared directly in EPR quartz tubes ( $d = 3$  mm) under normal atmosphere. EPR tubes were flushed with argon using a long needle for 2 minutes. The  $[\text{Ni}(\text{TMG}_3\text{tren})(\text{OTf})](\text{OTf})$  solution was prepared in the glove box and transferred to an EPR tube. The EPR tube was dipped in a cold bath kept at -30 °C and the temperature was allowed to be stabilized for 5 minutes. The *m*CPBA solution was prepared in the glove box and added to the cold complex solution via a syringe. Immediately after addition, the solution was stirred under argon flow for 0 – 2000

seconds; the sample was frozen by immersion in liquid nitrogen, and the EPR spectrum was measured at 10K.

For **kinetic EPR studies** substrates were directly added to the reaction mixture of **1-OTf** and *m*CPBA after 25 minutes of mixing in the EPR tube at -30 °C. To stop the reaction, the tube was again immersed in liquid nitrogen, followed by registration of the EPR spectrum at 10 K.

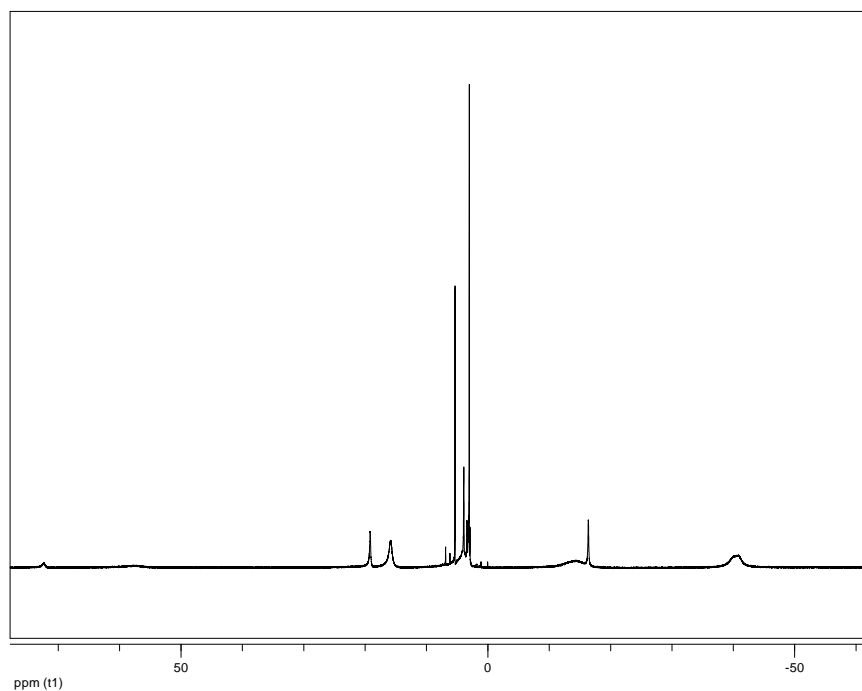


**Figure S1**  $^1\text{H}$ -NMR spectrum of **1-OTf** at 25 °C in  $\text{CD}_2\text{Cl}_2$ .

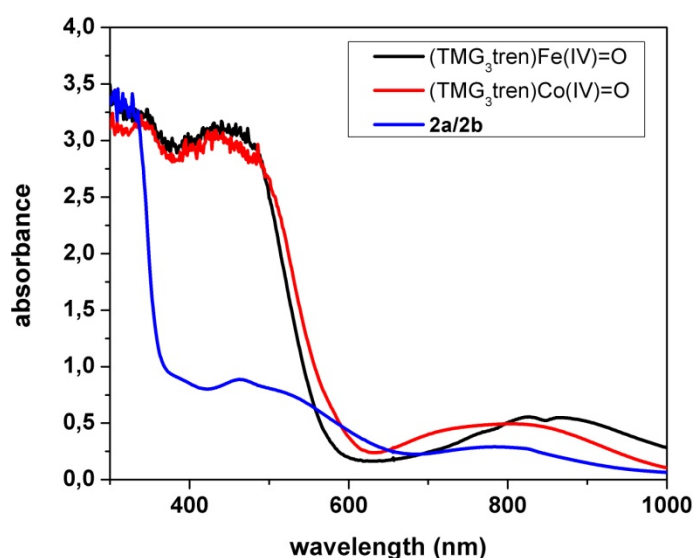


**Figure S2** Comparison of the UV/vis spectra of the previously reported<sup>6,7</sup> high valent  $(\text{TMG}_3\text{tren})\text{Fe}(\text{IV})=\text{O}$  (2.5 mM) and  $(\text{TMG}_3\text{tren})\text{Co}(\text{IV})=\text{O}$  (generated from 6 mM  $\text{Co}^{\text{II}}(\text{TMG}_3\text{tren})$ ; 60% yield of  $\text{Co}(\text{IV})$ ) complexes and the herein described Ni(III)- complexes **2a/2b** (generated from 2 mM **1-OTf**; 15 % yield of Ni(III)).

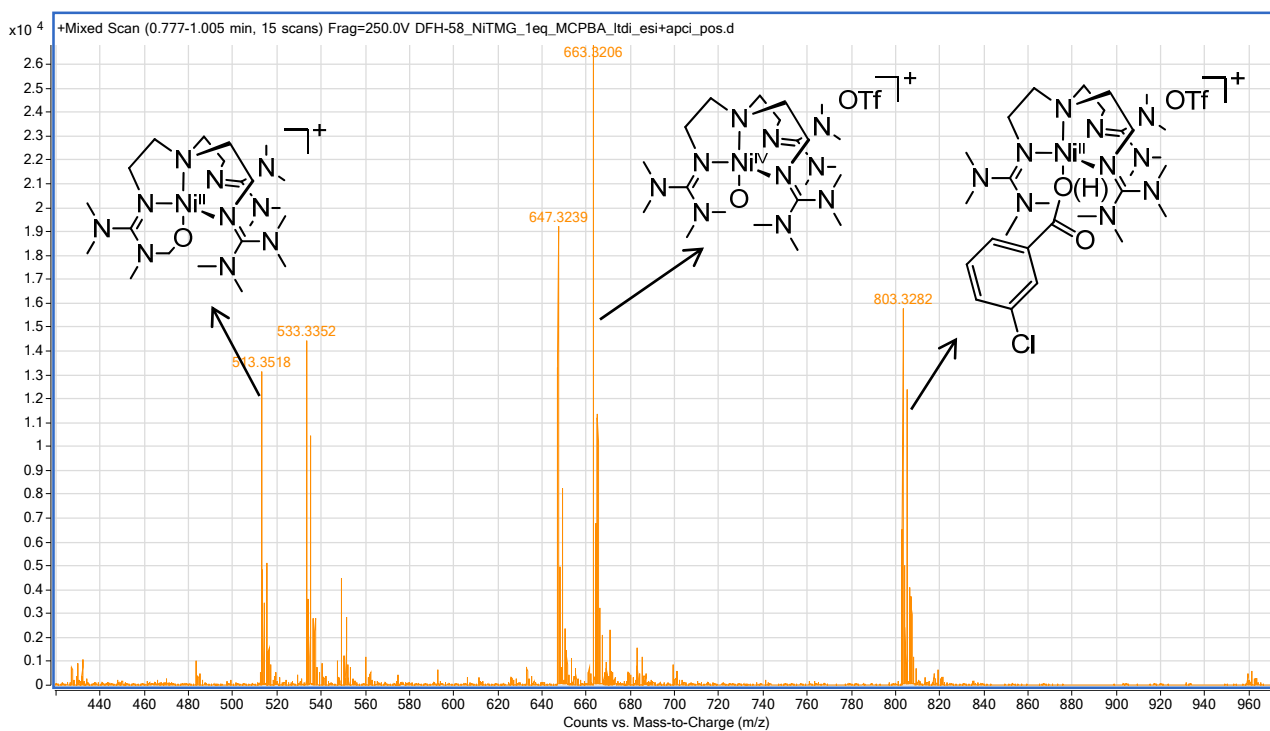


**Figure S3** ESI-MS spectrum of the reaction of **1-OTf** with 1 eq. *m*CPBA. Peaks in the spectrum are assigned to the alkoxonickel(II) complex  $[\text{Ni}^{\text{II}}(\text{O})(\text{TMG}_3\text{tren-H})]^+$  (found:  $m/z = 513.352$ , calc.:  $m/z = 513.329$ ), the nickel(II)chloro complex  $[\text{Ni}^{\text{II}}(\text{Cl})(\text{TMG}_3\text{tren})]^+$  (found:  $m/z = 533.335$ , calc.:  $m/z = 533.311$ ); the formation of the chloride complex results from the reaction of the triflate complex with the solvent ( $\text{CH}_2\text{Cl}_2$ ) under the ESI-MS conditions), **1-OTf** (found:  $m/z = 647.324$ , calc.:  $m/z = 647.294$ ), the  $[\text{Ni}^{\text{IV}}(\text{O})(\text{TMG}_3\text{tren})](\text{OTf})^+$  complex (found:  $m/z = 663.321$ , calc.:  $663.289$ ), and to the chlorobenzoic acid adduct  $[(\text{TMG}_3\text{tren})\text{Ni}^{\text{II}}(\text{HOC}(\text{O})\text{C}_6\text{H}_4\text{Cl})](\text{OTf})^+$  (found:  $m/z = 803.328$ , calc.:  $m/z = 803.292$ ).

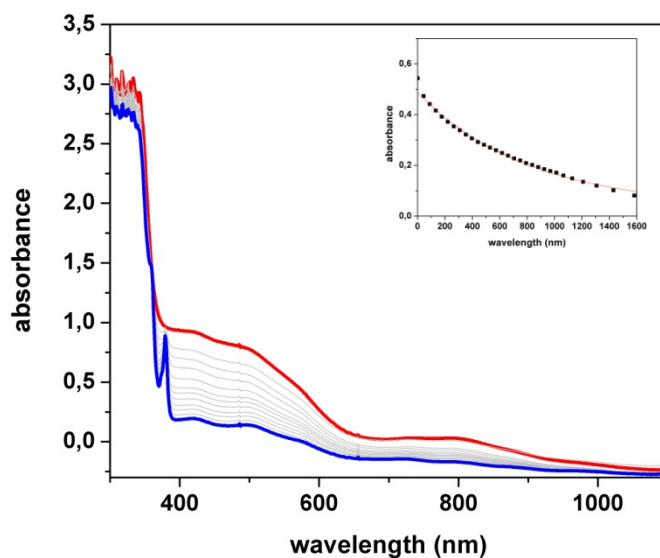


**Figure S4.** Change in the absorption spectra associated with the reaction of **2a/2b** with DHA (0.135 M) at -30 °C in CH<sub>2</sub>Cl<sub>2</sub>. In the inset is shown the pseudo-first order decay of the absorption band at 520 nm as a function of time.

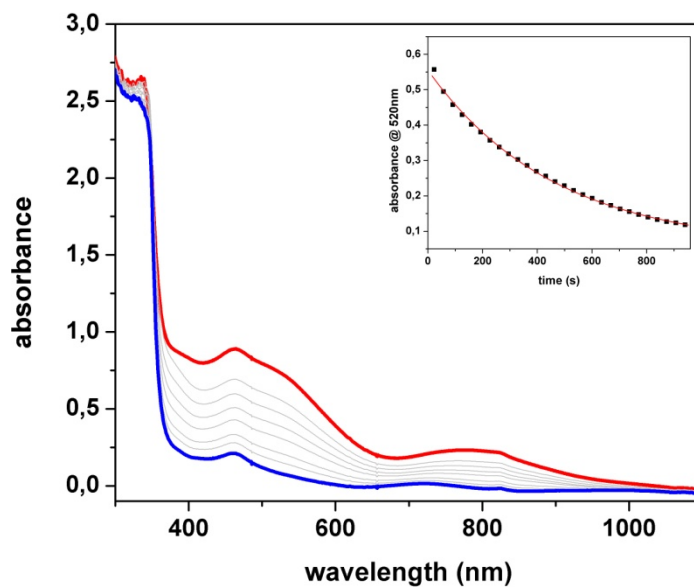


**Figure S5.** Change in the absorption spectra associated with the reaction of **2a/2b** with Xanthene (0.133 M) at -30 °C in CH<sub>2</sub>Cl<sub>2</sub>. In the inset is shown the pseudo-first order decay of the absorption band at 520 nm as a function of time.

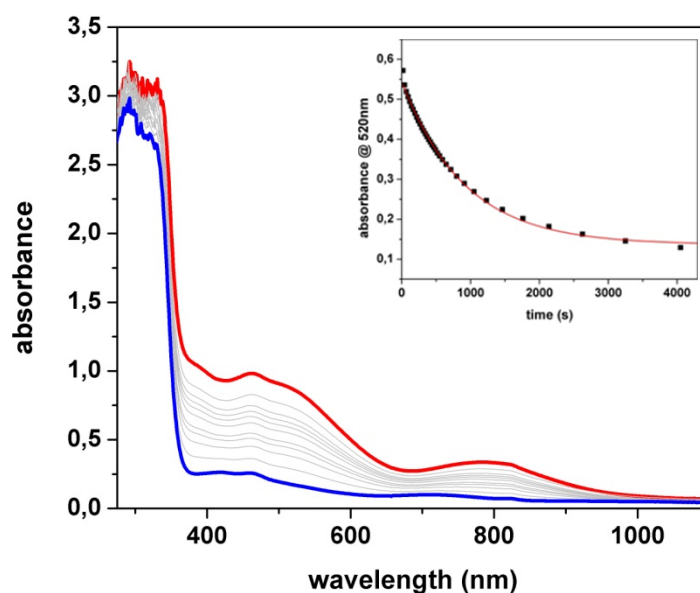


**Figure S6.** Change in the absorption spectra associated with the reaction of **2a/2b** with 1,4-cyclohexadiene (0.128 M) at -30 °C in CH<sub>2</sub>Cl<sub>2</sub>. In the inset is shown the pseudo-first order decay of the absorption band at 520 nm as a function of time.

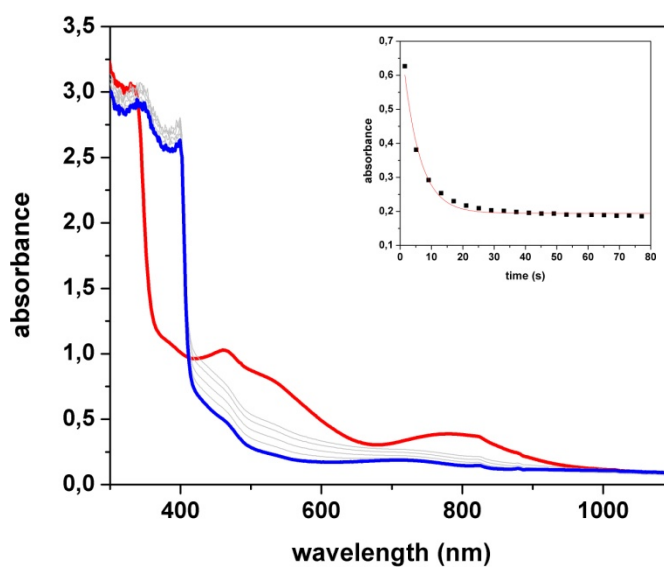


**Figure S7.** Change in the absorption spectra associated with the reaction of **2a/2b** with BNAH (0.027 M) at -60 °C in CH<sub>2</sub>Cl<sub>2</sub>. In the inset is shown the pseudo-first order decay of the absorption band at 520 nm as a function of time.



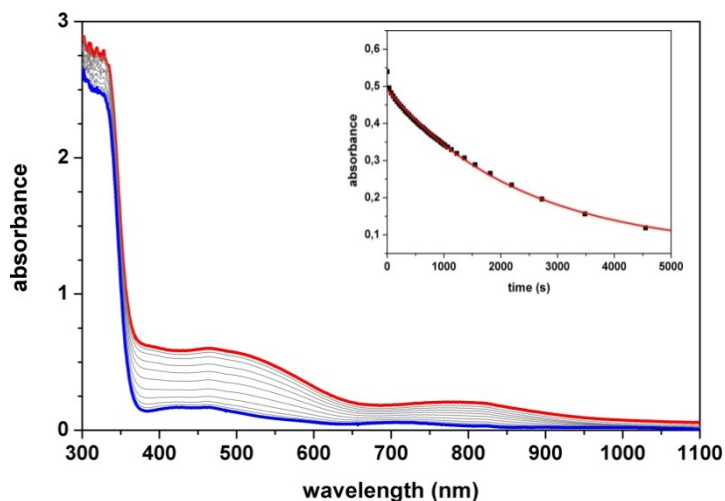


**Figure S8.** Change in the absorption spectra associated with the reaction of **2a/2b** with  $\text{PPh}_3$  (0.107 M) at  $-30\text{ }^\circ\text{C}$  in  $\text{CH}_2\text{Cl}_2$ . In the inset is shown the pseudo-first order decay of the absorption band at 520 nm as a function of time.

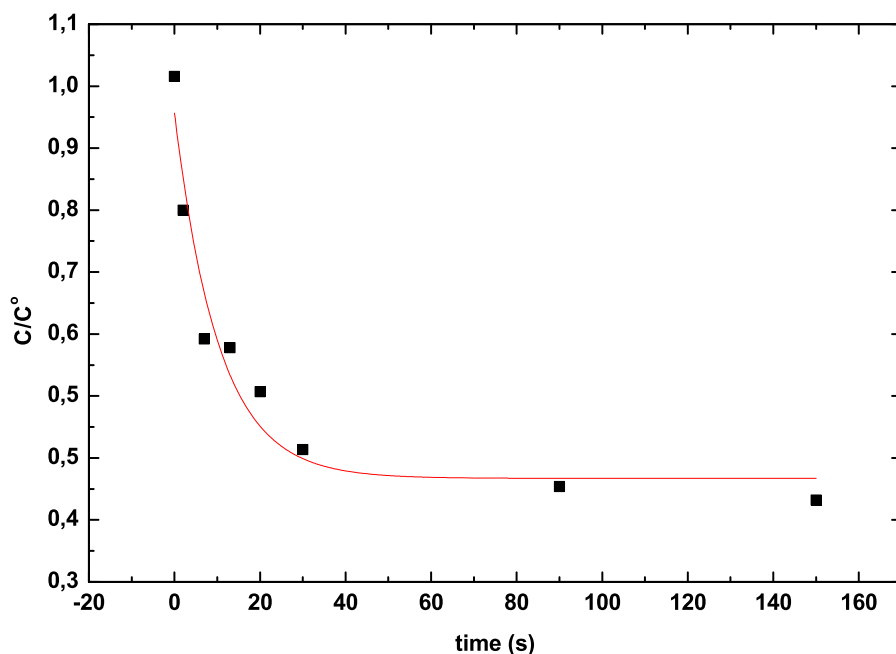


**Figure S9** Decay of the Ni(III)-EPR signal in presence of DHA in  $\text{CH}_2\text{Cl}_2$  at  $-30\text{ }^\circ\text{C}$ . The pseudo-first order fit of the decay is shown as a bold line.

#### Reference:

- [1] V. K. Aggarwal, Z. Gultekin, R. S. Grainger, H. Adams und P. L. Spargo, *J. Chem. Soc., Perkin Trans. 1*, 1998, **17**, 2771.
- [2] C. R. Goldsmith, R. T. Jonas, and T. D. P. Stack, *J. Am. Chem. Soc.*, 2002, **124**, 83.
- [3] A. L. Spek, *J. Appl. Cryst.*, 2003, **36**, 7.
- [4] G. M. Sheldrick, *Acta Cryst. A*, 2008, **64**, 112.
- [5] H. Wittmann, V. Raab, A. Schorm, J. Plackmeyer and J. Sundermeyer, *Eur. J. Inorg. Chem.*, 2001, **8**, 1937.

- [6] J. England, M. Martinho, E. R. Farquhar, J. R. Frisch, E. L. Bominaar, E. Münck and L. Que Jr., *Angew. Chem.*, 2009, **121**, 3676
- [7] F. F. Pfaff, S. Kundu, M. Risch, S. Pandian, F. Heims, I. Pryjomska-Ray, P. Haack, R. Metzinger, E. Bill, H. Dau, P. Comba and K. Ray, *Angew. Chem. Int. Ed.*, 2011, **50**, 1711.